Supporting Materials

Simultaneous Confocal Microscopy and Rheology Probes the Structural and Mechanical Evolution of Collagen I through the Sol-Gel Transition

Khanh-Hoa Tran-Ba[1], Daniel J. Lee[1], Jieling Zhu[1], Keewook Paeng[1,2], and Laura J. Kaufman[1,*]

[1]Department of Chemistry, Columbia University, 3000 Broadway, New York, NY 10027, USA

[2]current address: Department of Chemistry, Sungkyunkwan University (SKKU). Suwon, 440-746, Republic of Korea

* corresponding author: kaufman@chem.columbia.edu

Supporting Text 1: Control Gelation Experiments

We prepared control collagen samples (1.0 mg/ml) and gelled these samples at 25°C to confirm that the intrinsic collagen gelation characteristics were not perturbed by

1. confocal microscopy at low laser power
2. rheology at low (1%) strain and frequency (10 rad/s)
3. sample confinement (as imposed by the rheometer tool with a 0.1 mm truncation gap).

No perturbation was seen, as reflected by the similarity of crossover time (t_{CO}^{RHEO}), arrest time (t_{ARR}^{CRM}), and/or incorporation time (t_{INC}^{CFM}), shown in **Table S1**.

	t_{CO}^{RHEO}**(min ± SD)**	t_{ARR}^{CRM}**(min ± SD)**	t_{INC}^{CFM}**(min ± SD)**
Rheology only	11.1 ± 0.6	-	-
Rheology and Microscopy	10.6 ± 1.1	8.7 ± 0.6	17.1 ± 1.7
Confined Microscopy only	-	8.3 ± 0.3	17.2 ± 0.8
Unconfined Microscopy only	-	8.7 ± 0.6	17.5 ± 0.5

Table S1. Key Time Points Obtained from Different Collagen Gelation Interrogation Modes. Crossover time (t_{CO}^{RHEO}), arrest time (t_{ARR}^{CRM}), and incorporation time (t_{INC}^{CFM}) for data collected with rheology only (n = 24), simultaneous rheology and confocal microscopy (n = 9), confocal microscopy while confined on the rheometer (n = 3), and confocal microscopy of a thicker, unconfined sample gelled on the rheometer (n = 3). Two-tailed, unequal variance t-tests were performed to compare time points obtained from different interrogation methods. None were found to be statistically significantly different, with $p > 0.1$ for all comparisons.

Supporting Text 2: Summary of Frequency Dependence

Given potential frequency dependence of rheological measures as well as potential impact of rheology on gelation kinetics, we assessed time points of interest determined as a function of oscillatory rheology frequency. We found no dependence of these quantities on rheology frequency, as shown in **Table S2**.

ω (rad/s)	t_{CO}^{RHEO}	t_{CO}^{RHEO}	t_{ARR}^{CRM}	t_{INC}^{CFM}	r_{INF}^{CFM}	r_{INF}^{CRM}	I_{INF}^{CRM}	$d_{f,slice}$
0.5	10.9 ± 0.6	10.3 ± 0.4	8.7 ± 0.3	16.0 ± 1.0	11.4 ± 1.3	11.8 ± 1.3	14.0 ± 1.0	9.3 ± 1.1
1.0	11.1 ± 0.4	-	-	-	-	-	-	-
2.5	11.1 ± 0.3	10.8 ± 1.9	9.0 ± 1.0	18.3 ± 2.5	11.4 ± 1.8	11.4 ± 1.7	14.0 ± 1.5	8.9 ± 1.1
5.0	11.0 ± 0.8	-	-	-	-	-	-	-
10.0	11.2 ± 0.7	10.6 ± 1.0	8.7 ± 0.3	16.8 ± 0.3	10.9 ± 0.3	11.3 ± 0.5	12.8 ± 1.1	8.4 ± 1.4

Table S2. Key Time Points Determined from Measurements across Oscillatory Rheology Frequency, ω. Mean ± SD of n = 3 - 6 samples for 1.0 mg/ml collagen gelation at 25°C. Crossover time (t_{CO}^{RHEO}), arrest time (t_{ARR}^{CRM}), and incorporation time (t_{INC}^{CFM}), as well as inflection points (50% curve development) of CFM correlation coefficient (r_{INF}^{CFM}), CRM correlation coefficient (r_{INF}^{CRM}), CRM intensity (I_{INF}^{CRM}), and fractal dimension ($d_{f,slice}$) curves are assessed for measurements taken with rheology alone (first column only) and rheomicroscopy (other columns). No statistically significant differences were seen as a function of frequency, with all two-tailed, unequal variance t-tests across frequencies as well as those between crossover times for measurements with and without imaging yielding $p > 0.1$.

Supporting Text 3: Frequency Dependent Rheology and Penetration Depth

Frequency-dependent oscillatory rheology is commonly used to probe viscoelastic materials, though it is typically employed for materials at equilibrium rather than materials undergoing highly non-equilibrium processes such as the self-assembly studied in this work. In non-evolving systems, frequency dependence of storage and viscous moduli provides key insight into material properties. For example, scaling of storage and viscous moduli as $G' \sim \omega^2$ and $G'' \sim \omega$ is associated with a simple Maxwell model of a viscoelastic material. Frequency dependence exists in oscillatory rheology since the probing frequency interrogates behavior on particular timescales. A related point is that oscillatory rheology probes particular length scales, as described by Landau and

Lifshitz (1). Briefly, a solid body (such as the rheology cone) that is immersed in a viscous fluid and oscillates with frequency ω creates flow that generates a transverse wave that propagates in a direction perpendicular to its velocity,

$$v(x,t) = u_0 e^{-\sqrt{\frac{2\nu/\omega}{x}}} e^{-i\sqrt{\frac{2\nu/\omega}{x}-\omega t}}$$

with ν the kinematic viscosity of the fluid, ω the oscillatory rheology frequency, and u_o peak amplitude of the transverse wave. The amplitude of this wave, u_o, is exponentially damped by the fluid. This property can then be exploited to probe viscoelastic properties of a material over different length scales by varying the frequency of the tool's motion. The characteristic distance at which the amplitude of the transverse wave is damped by a factor of e is termed the penetration depth or characteristic length scale, $l_c = \left(\frac{2\nu}{\omega}\right)^{1/2}$ (1). For the frequency range interrogated here, the penetration depths are in the range of 1 – 5 mm using $\nu = 9 \times 10^{-7}$ m^2/s, the viscosity of water at 25ºC. These length scales are larger than all fiber dimensions and larger than the sample in the dimension perpendicular to the oscillation; thus, the frequencies employed probe length scales associated with the full axial dimension of the sample. The frequency independence of the crossover time that is seen in our study is therefore not unexpected since all frequencies used probe length scales associated with the presence of an (axially-) system spanning structure. To interrogate a shorter length scale, which could report on local entanglement of fibers before a system spanning structure is in place, a frequency of > 200 rad/s would be needed, as that frequency yields penetration depth of ≈ 250 nm, which is similar to the thickness of the sample at the imaging position. In this study, accessing such frequencies during self-assembly led to slip at the top tool, preventing interrogation of these length scales.

Supporting Text 4: Two and Three Dimensional Fractal Dimension

As described in the main text, there is no general relationship $d_{f,3D}$ and $d_{f,slice}$ for the Minkowski-Bouligand dimension. Because comparison to predictions of percolation theory requires knowledge of $d_{f,3D}$ while our measurements during gelation only capture $d_{f,slice}$, we analyzed 2D slices and 3D reconstructions from fully formed gels to find typical relationships between $d_{f,3D}$ and $d_{f,slice}$ in these systems. Assessment of 2D CRM and CFM images of fully formed collagen gels prepared at 25ºC and 37ºC was performed as described in Materials and Methods in the main text. Assessment of 3D reconstructions from slices of these same gels was performed as follows. Forty slice z-stacks with images collected every 1μm were recorded for fully-developed collagen networks. Each slice was thresholded using the isodata approach described in Materials and Methods in the main text. The 3D fractal dimension was then obtained in Fractal Count by converting the z-stack of 2D image slices into a 3D matrix and dividing the matrix into cubes for box-counting. The starting cube length was defined by the number of slices in the *z*-direction. Cubes of side 6 – 40 μm were then assessed through box-counting. A representative sample of a 1.0 mg/ml collagen sample formed at 25ºC is shown as a CFM stack and 3D reconstruction (**Fig. S1**), and a table of fractal dimensions obtained from 2D slices and 3D reconstructions is shown (**Table S3**). On average, we find $d_{f,3D} = d_{f,slice} + 0.92$.

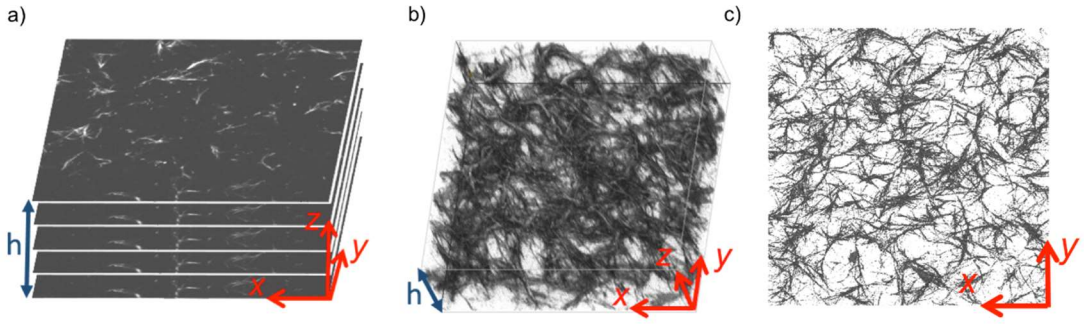

Figure S1. a) Subset of 2D CFM slices comprising a z-stack collected from a fully formed 1.0 mg/ml collagen gel assembled at 25ºC. b) 3D representation of the gel as reconstructed from the full z-stack covering 40 µm in the axial dimension. c) Top view of the same gel. Images in (b) and (c) were generated with the Volume Viewer in ImageJ.

T (°C)	$d_{f,slice}^{CRM}$	$d_{f,slice}^{CFM}$	$d_{f,3D}^{CRM}$	$d_{f,3D}^{CFM}$
25	1.67 ± 0.02	1.77 ± 0.03	2.60	2.70
37	1.81 ± 0.02	1.90 ± 0.02	2.73	2.81

Table S3. Fractal Dimension Determined from Fully Formed Gels Assembled at 25 and 37 °C. Mean ± SD of $d_{f,slice}$ analyzed from 40 slices of a 3D stack (two left columns) of a single sample prepared at 25ºC and another at 37ºC. $d_{f,3D}$ values determined from the same two samples.

Supporting Text 5: Statistical Tests Across Time Points

Time points summarized in **Table 1** in the main text were assessed with two-tailed, unequal variance t-tests. As expected, p-values were very small except for time points expected to be correlated, such as incorporation time, t_{INC}^{CFM}, and the plateau times of the correlation curves, r^{CFM} and r^{CRM}.

TIME		Arrest	Crossover	Incorp.	CFM Correlation Coefficient			CRM Correlation Coeffient			CRM Intensity			CRM Fractal dimension		
		t_{ARR}^{CRM}	t_{CO}^{RHEO}	t_{INC}^{CFM}	r^{CFM}			r^{CRM}			I^{CRM}			$d_{f,slice}$		
					LAG	INF	PL	LAG	INF	PL	LAG	INF	PL	LAG	INF	PL
t_{ARR}^{CRM}			8.77E-04	8.50E-05	3.26E-07	7.72E-05	4.46E-06	1.28E-04	2.05E-05	5.99E-07	1.41E-02	2.16E-07	4.44E-10	1.41E-09	7.49E-01	1.30E-07
t_{CO}^{RHEO}		8.77E-04		1.83E-07	2.92E-07	2.36E-01	2.32E-05	6.40E-07	9.08E-02	1.72E-06	2.88E-05	4.66E-05	1.25E-10	2.23E-11	5.05E-03	8.75E-07
t_{INC}^{CFM}		9.44E-08	1.83E-07		5.69E-09	6.51E-07	3.27E-01	2.29E-10	1.20E-06	7.62E-01	1.54E-09	1.97E-04	2.65E-03	4.51E-12	1.04E-08	8.18E-02
r^{CFM}	LAG	3.26E-07	2.92E-07	5.69E-09		6.30E-08	3.40E-07	8.46E-01	2.04E-08	4.37E-08	1.53E-02	1.70E-09	2.60E-11	1.53E-07	5.56E-05	4.37E-09
	INF	7.72E-05	2.36E-01	6.51E-07	6.30E-08		7.47E-05	1.03E-07	5.91E-01	5.63E-06	3.06E-06	5.29E-04	3.64E-10	7.76E-12	3.83E-04	4.57E-06
	PL	4.46E-06	2.32E-05	3.27E-01	3.40E-07	7.47E-05		4.94E-08	1.30E-04	5.01E-01	2.81E-07	1.13E-02	1.17E-03	1.35E-09	1.63E-06	6.08E-01
r^{CRM}	LAG	1.28E-04	6.40E-07	2.29E-10	8.46E-01	1.03E-07	4.94E-08		4.02E-08	3.17E-09	3.08E-02	6.08E-10	4.08E-13	7.82E-07	1.90E-04	2.48E-10
	INF	2.05E-05	9.08E-02	1.20E-06	2.04E-08	5.91E-01	1.30E-04	4.02E-08		3.10E-19	9.80E-07	1.42E-03	5.94E-10	3.68E-12	1.17E-07	9.45E-06
	PL	5.99E-07	1.72E-06	7.62E-01	4.37E-08	5.63E-06	5.01E-01	3.17E-09	3.10E-19		1.97E-08	1.08E-03	2.66E-03	8.36E-11	9.45E-06	1.84E-01
I^{CRM}	LAG	1.41E-02	2.88E-05	1.54E-09	1.53E-02	3.06E-06	2.81E-07	3.08E-02	9.80E-07	1.97E-08		6.57E-09	1.97E-12	1.25E-08	2.18E-02	2.04E-09
	INF	2.16E-07	4.66E-05	1.97E-04	1.70E-09	5.29E-04	1.13E-02	6.08E-10	1.42E-03	1.08E-03	6.57E-09		4.24E-08	4.50E-13	1.95E-07	6.61E-03
	PL	4.44E-10	1.25E-10	2.65E-03	2.60E-11	3.64E-10	1.17E-03	4.08E-13	5.94E-10	2.66E-03	1.97E-12	4.24E-08		8.88E-15	1.06E-11	2.42E-05
$d_{f,slice}$	LAG	1.41E-09	2.23E-11	4.51E-12	1.53E-07	7.76E-12	1.35E-09	7.82E-07	3.68E-12	8.36E-11	1.25E-08	4.50E-13	8.88E-15		1.06E-11	2.42E-05
	INF	7.49E-01	5.05E-03	1.04E-08	5.56E-05	3.83E-04	1.63E-06	1.90E-04	1.17E-07	9.45E-06	2.18E-02	1.95E-07	1.06E-11	1.06E-11		2.42E-05
	PL	1.30E-07	8.75E-07	8.18E-02	4.37E-09	4.57E-06	6.08E-01	2.48E-10	9.45E-06	1.84E-01	2.04E-09	6.61E-03	2.42E-05	2.42E-05	2.42E-05	

Table S4. p-values obtained from t-tests. p values obtained from two-tailed, unequal variance t-tests across all time points summarized in **Table 1**. Those with $p > 0.1$ are highlighted in red.

Video S1: Video showing simultaneous rheology (left panel), CFM (center panel) and CRM (right panel) recorded during gelation of a 1.0 mg/ml collagen gel self-assembling at 25°C. This sample is the same sample from which the images in Fig. 2 and Fig. 5 in the main text are obtained. The storage, G', and loss, G", moduli were measured at 10.0 rad/s. Each point in oscillatory rheology was collected and averaged over 15s and interval between images was also 15s. Playback speed is 1 frame/s. The video reflects data recorded at $t = 7 – 27$ min.

Reference

1. Landau, L.D., and E.M. Lifschitz. 1987. Fluid Mechanics. Second Ed. Burlington: Butterworth-Heinemann.